IOPscience iopscience.iop.org

Home Search Collections Journals About Contact us My IOPscience

One-dimensional probability density observed using scanned gate microscopy

This article has been downloaded from IOPscience. Please scroll down to see the full text article.

2000 J. Phys.: Condens. Matter 12 L735

(http://iopscience.iop.org/0953-8984/12/50/102)

View the table of contents for this issue, or go to the journal homepage for more

Download details:
IP Address: 171.66.16.226
The article was downloaded on 16/05/2010 at 08:13

Please note that terms and conditions apply.

J. Phys.: Condens. Matter **12** (2000) L735–L740. Printed in the UK PII: S0953-8984(00)18094-4

LETTER TO THE EDITOR

One-dimensional probability density observed using scanned gate microscopy

R Crook, C G Smith, M Y Simmons† and D A Ritchie

Department of Physics, Cavendish Laboratory, Madingley Road, Cambridge CB3 OHE, UK

E-mail: rc230@cam.ac.uk (R Crook)

Received 18 October 2000

Abstract. Using scanned gate microscopy, we observed transconductance structure relating to the transverse electron probability density of a quasi-one-dimensional electron system (Q1DES). The scanned gate created a movable scatterer to modify the transmission probability of the highest transmitted one-dimensional (1D) subband. Structure was seen for the first three 1D subbands, in addition to transconductance oscillations indicative of 1D ballistic transport. The Q1DES was electrostatically defined from a subsurface two-dimensional electron system created at a GaAs/AlGaAs heterojunction. The Q1DES confining potential was modelled as flat in the middle with parabolic walls, and Schrödinger's equation solved numerically using a finite-difference method. Using this model, the experimental Q1DES width and 1D subband energy spacings were deduced.

Scanned gate microscopy studies the conducting properties of a sample by scanning a biased probe over the sample surface and recording the changing sample conductance [1–6]. The resulting images are a convolution of the probe electric perturbation and a spatial map of the sample response. The scanning probe is usually a conducting atomic force microscope (AFM), enabling topographic images to identify surface features such as gate electrodes. Scanned gate microscopy has recently been used to study electronic transport through constrictions [1], quasi-1D systems [2–4], 2D systems [5], and carbon nanotubes [6]. These experiments have proved particularly successful for studying the effects of defects and disorder.

The discovery of 1D ballistic quantization [7, 8] demonstrated the role of 1D subbands in determining conductance of quasi-1D electron systems (Q1DES). The conductance of a Q1DES is $(2e^2/h)\sum T_n$ where T_n is the transmission probability of subband n assuming no intersubband scattering. By positioning a charged probe in the 2D region adjacent to a Q1DES [4], backscattering has been shown to modify T_n. Subsequent images, made by recording Q1DES conductance as the probe scanned, revealed the injected electron flux. Such images are a projection of the total probability density at the Q1DES exit. Probability densities of a Q1DES have also been studied by scanning a Q1DES over a sharp potential [10]. The Q1DES was scanned by applying asymmetric biases to surface gates which defined the system. The sharp potential was assumed to originate from a random impurity, although the potential shape was unknown.

In this letter we report a scanned gate microscopy experiment made to investigate transverse 1D electron probability density with a spatial resolution less than the electron 1D wavelength. A charged tip was positioned at a series of points across the width

† Present address: School of Physics, University of New South Wales, Sydney 2052, Australia.

0953-8984/00/500735+06$30.00 © 2000 IOP Publishing Ltd

of an electrostatically defined Q1DES. At each point the Q1DES width was swept, varying the number of transmissive 1D subbands. Strong oscillations observed in Q1DES transconductance, and associated conductance plateaus quantized in units of $2e^2/h$, confirmed the 1D nature of the device. Additional structure was observed across the width of the Q1DES, which we interpret as relating to the 1D probability density. Backscattering did not occur for the 1D subbands below the Fermi energy because only a small bias was applied to the tip which was positioned over, and not adjacent to, the Q1DES. The data are related to the probability density of the 1D subband closest to the Fermi energy.

It is generally accepted that for the first subband, the 1D confining potential can be approximated as a parabola. For higher subband occupation, a confining potential with a flat bottom and parabolic walls is more realistic. For such a 1D potential, Schrödinger's equation was solved numerically using a finite-difference method to predict the eigenfunction and eigenenergies. By equating the experimental peaks in transconductance to the theoretical peaks in probability density, the Q1DES width and 1D subband spacings are deduced for the second, third, and fourth subbands.

The device was a GaAs/AlGaAs heterostructure incorporating a 2D electron system (2DES) 98 nm beneath the surface. The layer from 40 nm to 80 nm above the 2DES was doped with Si at a concentration of 1.2×10^{18} cm^{-3}. By applying a negative bias to Au/NiCr surface electrodes, underlying 2DES electrons were repelled to define the Q1DES. The surface electrodes were patterned in a split-gate configuration with a lithographic gate width of 700 nm and length of 800 nm. Source and drain ohmic contacts to the 2DES provided electrical connections to the Q1DES. The final processing stage made an alignment grid on the device surface.

A low-temperature atomic force microscope (AFM) imaged the alignment grid to locate the split-gate surface electrodes. The tip-to-surface force measurement was made using commercial piezoresistive cantilevers [11]† proving ideal for operation at low temperatures over light-sensitive semiconductor devices. During subsequent electrical measurements, the AFM operated as a scanning charged probe by applying an AC signal to a resistive path connecting to the conductive AFM tip. The tip was positioned approximately 10 nm off the device surface to ensure that no charge flowed between the tip and the device. These experiments were performed at 4.2 K, the device and the AFM being submerged in liquid ^{4}He.

Figure 1 plots the device conductance against gate bias. Plateaus quantized in units of approximately $2e^2/h$ demonstrate the 1D nature of the device. Higher plateaus are quantized in units less than $2e^2/h$ because the data have not been corrected for the series resistance from wires, contacts, and the 2DES.

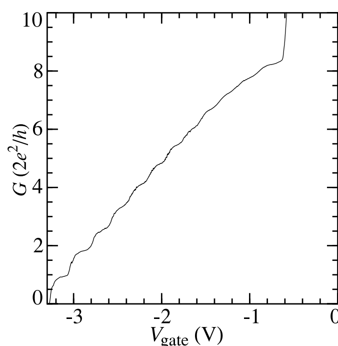

Figure 1. An experimental plot of Q1DES conductance against gate bias. The conductance is quantized in units of approximately $2e^2/h$. These data have not been corrected for a series resistance.

† Park Scientific Instruments, Sunnyvale, CA 94089, USA.

Figure 2 presents a contour plot of processed experimental data. A low-frequency AC signal of 0.5 V_{rms} was applied to the tip, and a DC bias of 1 mV applied to the Q1DES source. The AC Q1DES drain current was measured with a lock-in amplifier. The charged tip was positioned at a series of points across the width of the Q1DES, providing the y_{tip}-axis of figure 2. At each point the Q1DES transconductance $\partial G/\partial V_{tip}$ was recorded, while the gate bias V_{gate} was swept from -2 V to Q1DES pinch-off which occurred at -3.5 V. A smoothing procedure was used to reduce the effects of noise, so extracting information from many data points. Measurements made from just the maximum transconductance would sample fewer data points and therefore be subject to increased noise. The data in figure 2 was linearly interpolated in the y_{tip}-direction.

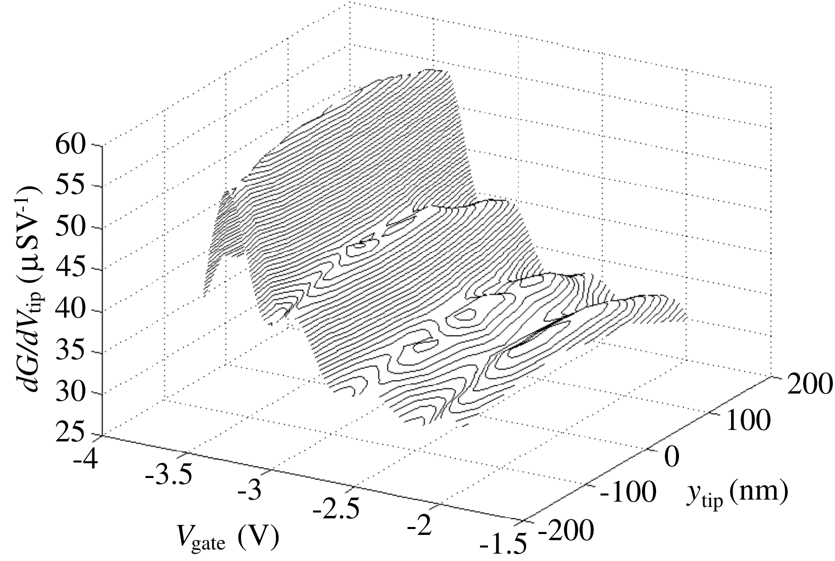

Figure 2. An experimental contour plot of the Q1DES transconductance. The gate bias was swept with the tip positioned at a series of points across the width of the Q1DES.

Transconductance, in figure 2, reveals structure with both V_{gate} and y_{tip}. The strong oscillations with V_{gate} arise from the gradient of quantized conductance shown in figure 1. A trough in these oscillations corresponds to a plateau in 1D quantized conductance. The next 1D subband becomes transmissive as the subband eigenenergy crosses the Fermi level. This is observed as a peak in the strong oscillations. Much weaker transconductance modulation with y_{tip} is observed superimposed on the peaks with V_{gate}. One, two, three, and possibly four peaks are seen with y_{tip} occurring at the onset of the first, second, third, and fourth subbands respectively. This structure is interpreted as being related to the probability density of individual 1D modes.

The transconductance measurement can be understood by first considering a DC measurement of Q1DES conductance G which is a function of the tip bias V_{tip}, the tip position y_{tip}, and the Fermi energy E_F. For a small tip bias δV_{tip}, the DC measurement can be written as

$$G = G_0 + \delta E_n \frac{\mathrm{d}G_0}{\mathrm{d}E_F} \tag{1}$$

where G_0 is the Q1DES conductance when $V_{tip} = 0$ V. The small change in eigenenergy δE_n, which is function of y_{tip}, is due to δV_{tip}. In the experiment an AC measurement of conductance,

or transconductance, was made. This measurement can be written as

$$\frac{\partial G}{\partial V_{\text{tip}}} = \frac{\delta E_n}{\delta V_{\text{tip}}}\frac{\mathrm{d}G_0}{\mathrm{d}E_F}. \tag{2}$$

In figure 2, the strong oscillations with V_{gate} are due to the $\mathrm{d}G_0/\mathrm{d}E_F$ term in equation (2). The gate bias modifies the shape of the confining potential and therefore E_F. Note that the assumption that this is a linear relationship is not realistic near Q1DES pinch-off [15]. In figure 2, the weak modulation with y_{tip} is due to the change in the $\delta E_n/\delta V_{\text{tip}}$ term as a function of y_{tip} in equation (2). In the following discussion it is shown that δE_n relates to the probability density of subband n. Therefore, this experiment is only sensitive to the probability density of the 1D subband closest to the Fermi energy, through modification to T_n. The lower-energy subbands are fully transmissive and do not contribute to the transconductance measurement.

A sufficiently local perturbation in the 1D confining potential results in a variation of the 1D eigenenergy perturbation with tip position, which relates to the associated probability density. When the tip is positioned over a maximum in the probability density for subband n, the perturbation is maximum. This modifies the transmission probability of subband n, so changing the conductance as the subband is depopulated.

To interpret the structure with y_{tip} seen in figure 2, the device is modelled as an infinitely long Q1DES. The 1D confining potential $U(y)$ consists of a flat region of width t bounded by parabolic walls with a curvature set by ω_0, which is sometimes described as a bathtub potential:

$$2U(y) = \begin{cases} m^\star\omega_0^2(|y| - t/2)^2 & \text{when } |y| > t/2 \\ 0 & \text{elsewhere} \end{cases} \tag{3}$$

where $m^\star$ is the electron effective mass in GaAs. This potential has been shown to be realistic for surface gated devices similar to those used in this experiment [12–14], although a parabolic confining potential is a better model for the first subband. The 1D eigenenergies and eigenfunctions were predicted by numerically solving Schrödinger's equation using a finite-difference method. The probability density of subband n exhibits n peaks in the y-direction. Figure 3(a) plots the confining potential, eigenenergies, and probability density when eigenenergy E_3 is at the Fermi level. Note that the shape of the confining potential, probability densities and eigenenergies will be different when the other subbands cross the Fermi level.

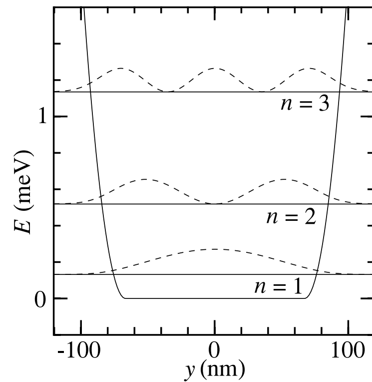

Figure 3. The model confining potential (solid), eigenenergy (solid), and probability density (dotted) for the first three 1D subbands.

Figure 4 shows the result of a first-order perturbation theory calculation for $n = 2$. The change to the eigenenergy δE_n is the convolution of the probability density with the tip potential. The tip potential is assumed to originate from a point charge $\alpha(d^2 + r^2)^{-0.5}$ where

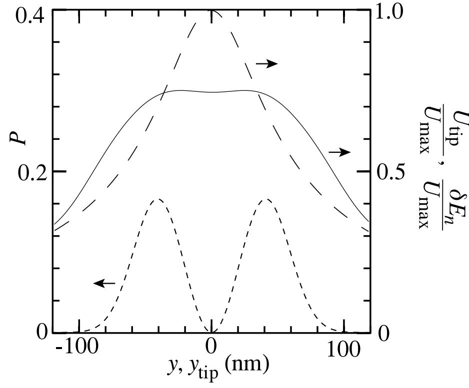

Figure 4. The probability density for $n = 2$ (dotted), model tip perturbing potential (dashed), and first-order eigenenergy change for $n = 2$ as a function of the tip position (solid). U_{max} is the peak tip perturbation.

α is a constant, d is the distance from the point charge to the 2DES, and r is the radial distance from the point charge in the 2DES plane. Figure 4 predicts that structure in δE_2 is only resolved when $d < 40$ nm. However, the tip to 2DES separation is greater than 100 nm. The enhanced resolution is interpreted as a screening effect from the donors, possibly forming a parallel conducting layer, which are located from 40 nm above the 2DES plane. Screening is known to sharpen the potential of a point charge [16]. Work involving a double 2DES has shown that screening from a parallel layer is possible despite as immeasurably small net current flow [17].

To determine t_n and the 1D subband energy spacing ΔE_n, the experimental transconductance peak positions with y_{tip} were equated to the theoretical positions. The experimental positions were measured on peaks with V_{gate} where the 1D eigenenergy crossed the Fermi level. The parabolic confining walls were assumed to extend 25 nm from the bottom of the confining potential to the Fermi level. The width of the confining potential was varied till the experimental and theoretical peaks coincided.

Twice the peak separation determines the 1D electron wavelength. From figure 2 the 1D wavelengths λ_n are $\lambda_2 = 160 \pm 10$ nm, $\lambda_3 = 140 \pm 10$ nm, and $\lambda_4 = 120 \pm 10$ nm. Using this technique, λ_1 cannot be determined. The 1D wavelength depends upon the shape of the 1D confining potential. It is not directly related to the 2D Fermi wavelength which in this case is $\lambda_F \approx 50$ nm. It is informative to compare these wavelengths with those obtained from a previous experiment where the Q1DES was scanned over a sharp defect potential [10], which were $\lambda_1 \approx 200$ nm, $\lambda_2 \approx 150$ nm, $\lambda_3 \approx 120$ nm, and $\lambda_4 \approx 110$ nm. These wavelengths differ from those calculated in this letter due to different carrier concentrations and different confinement potentials.

In table 1, t_n and ΔE_n are calculated from the theoretical fit for $n = 2, 3$, and 4. Note that the energy spacing is obtained at the onset of a subband, and not between two subbands

Table 1. Q1DES width and 1D subband spacing, determined by fitting experimental and theoretical peak transconductance positions.

n	Experimental peak positions (nm)	Calculated t_n (nm)	Calculated ΔE_n (meV)
1	0		
2	-40 ± 5, $+40 \pm 5$	78 ± 10	0.62 ± 0.07
3	-70 ± 10, 0, $+70 \pm 10$	131 ± 10	0.61 ± 0.07
4	-90 ± 10, -30 ± 5, $+30 \pm 5$, $+90 \pm 10$	161 ± 10	0.69 ± 0.07

as would be obtained in a DC source–drain bias experiment [15]. The uncertainties quoted in table 1 are derived from experimental error and do not include inaccuracies due to the theoretical model. This experiment was performed at 4.2 K where $k_B T = 0.36$ meV.

In conclusion, we have used a scanning charged probe to observe structure relating to the transverse probability density of a quasi-1D electron system (Q1DES). Oscillations were observed in the transconductance with gate bias, corresponding to quantized plateaus in conductance, confirming the 1D nature of the Q1DES. Structure was observed in the transverse direction transconductance which was related to the 1D probability density. By assuming a bathtub confining potential, electron 1D wavelengths, the shape of the confining potential, and 1D subband energy spacings were deduced for the second, third, and fourth subbands.

We thank C H W Barnes for the numerical solution program. We acknowledge financial support from the EPSRC and the R W Paul Instrument Fund.

References

[1] Eriksson M A, Beck R G, Topinka M, Katine J A, Westervelt R M, Campman K L and Gossard A C 1996 *Appl. Phys. Lett.* **69** 671

[2] Crook R, Smith C G, Simmons M Y and Ritchie D A 1999 *Proc. 24th Int. Conf. on The Physics of Semiconductors (Jerusalem)* ed D Gershoni (Singapore: World Scientific) p 190

[3] Crook R, Smith C G, Barnes C H W, Simmons M Y and Ritchie D A 2000 *J. Phys.: Condens. Matter* **12** L167

[4] Topinka M A, LeRoy B J, Shaw S E J, Heller E J and Westervelt R M 2000 *Science* **289** 2323

[5] Crook R, Smith C G, Simmons M Y and Ritchie D A 2000 *Phys. Rev.* B **62** 5174

[6] Bachtold A, Fuhrer M S, Plyasunov S, Forero M, Anderson E H, Zettl A and McEuen P L 2000 *Phys. Rev. Lett.* **84** 6082

[7] van Wees B J, van Houten H, Beenakker C W J, Williamson J G, Kouwenhoven L P, van der Marel D and Foxon C T 1988 *Phys. Rev. Lett.* **60** 848

[8] Wharam D A, Pepper M, Ahmed H, Frost J E F, Hasko D G, Peacock D C, Ritchie D A and Jones G A C 1988 *J. Phys.: Solid State Phys.* **21** L887

[9] Laux S E and Stern F 1986 *Appl. Phys. Lett.* **49** 91

[10] Williamson J G, Timmering C E, Harmans C J P M, Harris J J and Foxon C T 1990 *Phys. Rev.* B **42** 7675

[11] Tortonese M, Barret R C and Quate C F 1993 *Appl. Phys. Lett.* **62** 834

[12] Laux S E, Frank D J and Stern F 1988 *Surf. Sci.* **196** 101

[13] Wharam D A, Ekenberg U, Pepper M, Hasko D G, Ahmed H, Frost J E F, Ritchie D A, Peacock D C and Jones G A C 1989 *Phys. Rev.* B **39** 6283

[14] Kardynal B, Barnes C H W, Linfield E H, Ritchie D A, Nicholls J T, Brown K M, Jones G A C and Pepper M 1997 *Phys. Rev.* B **55** R1966

[15] Thomas K J, Simmons M Y, Nicholls J T, Mace D R, Pepper M and Ritchie D A 1995 *Appl. Phys. Lett.* **67** 109

[16] Ando T, Fowler A B and Stern F 1982 *Rev. Mod. Phys.* **54** 437

[17] Field M, Smith C G, Pepper M, Brown K M, Linfield E H, Grimshaw M P, Ritchie D A and Jones G A C 1996 *Surf. Sci.* **362** 154